HHS Public Access

Author manuscript

Soft Matter. Author manuscript; available in PMC 2016 December 19.

Published in final edited form as:

Soft Matter. 2016 May 07; 12(17): 3854–3859. doi:10.1039/c6sm00268d.

Instabilities, defects, and defect ordering in an overdamped active nematic†

Elias Putzig[a,‡], **Gabriel S. Redner**[a], **Arvind Baskaran**[b], and **Aparna Baskaran**[a]

[a]Martin Fisher School of Physics, Brandeis University, Waltham, MA 02453, USA

[b]Department of Chemistry and Biochemistry, University of Maryland, College Park, MD 20742, USA

Abstract

We consider a phenomenological continuum theory for an extensile, overdamped active nematic liquid crystal, applicable in the dense regime. Constructed from general principles, the theory is universal, with parameters independent of any particular microscopic realization. We show that it exhibits two distinct instabilities, one of which arises due to shear forces, and the other due to active torques. Both lead to the proliferation of defects. We focus on the active torque bend instability and find three distinct nonequilibrium steady states including a defect-ordered nematic in which $+\frac{1}{2}$ disclinations develop polar ordering. We characterize the phenomenology of these phases and identify the relationship of this theoretical description to experimental realizations and other theoretical models of active nematics.

Introduction

Liquid crystals are anisotropic fluid mesophases that exhibit broken rotational symmetry and have been extensively studied for many years[1]. The study of topological defects in the orientational order in these systems, which typically occur under driving, has had a central role in developing our understanding of the material properties of these systems[2,3]. *Active* liquid crystals are driven at the scale of the microscopic nematogen, and the microscale internal forces give rise to spontaneous nucleation of defects and novel defect dynamics[4–7].

One system, composed of cytoskeletal filaments driven by motor proteins[4–6] confined to a fluid interface, has inspired much theoretical effort to understand its dynamics[6,8–19]. These theories show how fluid mediation, in the form of active and passive backflow, can lead to the formation and propulsion of defects. However, these nonequilibrium phenomena also arise in active nematic systems in which fluid mediation plays little or no part, such as vibrated monolayers of granular rods[20], epithelial cell monolayers[21], and elongated fibroblasts[22]. It must therefore be possible to describe these systems with overdamped dynamics, in which activity is transmitted directly, rather than through the mediation of a fluid.

†Electronic Supplementary Information (ESI) available: See DOI: 10.1039/b000000x/

‡ efputzig@brandeis.edu.

In this work we develop a phenomenological continuum theory that describes the dynamics of an overdamped active nematic in two dimensions, and is applicable to all systems in this symmetry class. This theory contains two mechanisms through which the active forces give rise to instabilities in the homogeneous nematic state in the dense regime. One is analogous to the instability due to flow alignment in fluid-mediated theories[11,13,23], in that it arises due to reorientation of the director under shear. The other is an instability that arises due to rotation of the director by internal forces in an active nematic.

We unfold the rich phenomenology that emerges due to the active torque instability in the numerical investigation, focusing on extensile systems in the dense regime. The nonequilibrium steady-states that we find are (i) a defect-ordered nematic that exhibits emergent polar ordering of $+\frac{1}{2}$ defects, (ii) a defect-free undulating nematic (see Fig. 1 and ESI†), and (iii) a defective, turbulent nematic (see Fig. 2).

The appearance of a defect-ordered state is of particular interest, as defect-ordering was recently discovered in layers of active cytoskeletal filaments and in simulations of overdamped extensile rigid rods[6]. While the long-range ordering of defects in these states is reminiscent of blue phases[24] and twist-grain-boundary phases[25] in equilibrium liquid crystals, the defect-ordered states in the active systems differ in that the defects themselves are motile and transient rather than existing in a static lattice.

The defect ordering in the experiment had nematic symmetry, while simulations displayed the same polar symmetry that we observe. We show that polar ordering of defects is a metastable state that occurs *below the threshold for any instability of the homogeneous nematic state* and depends on the breaking of Galilean invariance in the overdamped limit. Further, we identify the relationship of our approach to other theories in the literature.

Theoretical Framework

An equilibrium nematic is described by the well-known Landaude Gennes free energy $\mathscr{F}$ that is a functional of the density $\rho(\vec{r}, t)$ and the nematic order tensor, $\mathbf{Q}(\vec{r}, t)$, associated with rotational symmetry breaking[1,26]. Its dynamics is given by gradient descent on this free energy landscape: 'Model A' dynamics for the director, $\partial_t \mathbf{Q}(\vec{r}) = -\gamma^{-1}\frac{\delta \mathscr{F}}{\delta \mathbf{Q}(\vec{r})}$, and 'Model B' dynamics for the conserved density field, $\partial_t \rho(\vec{r}) = -\gamma'^{-1}\nabla^2\frac{\delta \mathscr{F}}{\delta \rho(\vec{r})}$. For an active nematic, however, microscopic forces exerted by the constituent particles can give rise to dynamics that are not integrable, and are therefore inherently nonequilibrium.

We shall consider the dynamics of systems of extensile particles, which push along their long axes, acting as force dipoles. The forces exerted by the particles cause a stress $\boldsymbol{\sigma} = f\mathbf{Q}$[§]. In a flat nematic these forces are locally balanced and the stress is exerted only on the boundary. When there is a local distortion of the order, however, there is a net force $F \propto -\vec{\nabla}$

[§] f is positive (negative) if the particles are extensile (contractile)

$\cdot \mathbf{Q}$ from this stress. This force can lead to a flow of particles $\rho\vec{u} = -\vec{F}/\xi$ (where ξ is a friction coefficient). We *postulate* that an active liquid crystal undergoes gradient descent dynamics in the local rest frame of a *self-generated flow arising from the activity*.

The flows which we consider are the motions of particles which reside near some surface, and in which neighboring particles are pushing on each other. We will therefore use a generalized form of the Beris-Edwards equations[26], which describe how flow modifies the gradient descent dynamics of particles which are suspended in fluid when they interact solely through stresses in the fluid.

$$\partial_t \rho = -\gamma'^{-1}\nabla^2 \frac{\delta \mathscr{F}}{\delta \rho(\vec{r})} - \vec{\nabla}\cdot\rho\vec{u} \quad (1)$$

$$\partial_t \mathbf{Q} + \lambda_C^- \vec{\nabla}\cdot\vec{u}\mathbf{Q} = -\gamma^{-1}\frac{\delta \mathscr{F}}{\delta \mathbf{Q}} + \lambda_R^-(\mathbf{Q\Omega} - \mathbf{\Omega Q}) + \lambda_1 \mathbf{E}^{\mathscr{T}} + \lambda_2(\mathbf{QE} + \mathbf{EQ})^{\mathscr{T}} \quad (2)$$

where $\mathbf{\Omega}_{ij} = \frac{1}{2}(\frac{\partial}{\partial x_i}u_j - \frac{\partial}{\partial x_j}u_i)$ is the vorticity tensor, $\mathbf{E}_{ij} = \frac{1}{2}(\frac{\partial}{\partial x_i}u_j + \frac{\partial}{\partial x_j}u_i)$ is the strain-rate tensor associated with the flow, λ_1 and λ_2 are the first and second-order flow-alignment parameters, and $(\mathbf{A})^{\mathscr{T}}$ denotes the traceless version of $\mathbf{A}$ (e.g. $\mathbf{A} - \frac{1}{2}\mathrm{Tr}(\mathbf{A})\mathbf{I}$).

The dynamical equations above are a generalization of the Beris-Edwards dynamical equations in that the equations above are not coupled to the flow of an incompressible medium, and in that these equations allow for broken Galilean invariance through the inclusion of coefficients in front of the convective and rotational terms, $\bar{\lambda}_C$ and $\bar{\lambda}_R$ respectively. It is relevant to consider an effectively compressible flow on a two-dimensional surface, as fluid can be pushed out into the third dimension. Also, in an overdamped system which is moving with respect to a fixed substrate, Galilean invariance may be broken, as that surface provides a reference frame. This generalization is also logical in the case of particles which are in direct contact, rather than suspended and interacting purely through a fluid. Broken Galilean invariance has been shown to make a significant difference in the dynamics of active polar fluids[27–31], but its consequence for a fluid of nematic symmetry has not been considered in existing literature.

When the flow from the active forces $\rho\vec{u} = -\frac{f}{\xi}\vec{\nabla}\cdot\mathbf{Q}$ is replaced in Eqs. 1 and 2, the dynamical equations for an active nematic take the form

$$\partial_t \rho = D\nabla^2\rho + D_Q \nabla\nabla{:}\mathbf{Q} \quad (3)$$

$$\partial_t \mathbf{Q} = -\gamma^{-1}\frac{\delta \mathscr{F}}{\delta \mathbf{Q}} + \frac{\lambda_C}{\rho}[\overrightarrow{\nabla \mathbf{Q}}]\cdot\overrightarrow{\nabla}\mathbf{Q} - \frac{\lambda_S}{2\rho}\mathbf{Q}(\nabla\nabla{:}\mathbf{Q}) - \frac{\lambda_R}{\rho}(\mathbf{Q}\cdot\nabla\nabla\cdot\mathbf{Q} - \overrightarrow{\nabla}(\overrightarrow{\nabla \mathbf{Q}})\cdot\mathbf{Q})^{\mathscr{S}} - \lambda_E\nabla^2\mathbf{Q} \quad (4)$$

where $\mathbf{A} : \mathbf{B} = A_{ij}B_{ij}$, and $\mathscr{S}$ denotes symmetrization (i.e. $(\mathbf{A})^{\mathscr{S}} = \frac{1}{2}(\mathbf{A}+\mathbf{A}^{\mathbf{T}})$)

The self-generated flow enters through the curvature induced density flux (CIDF), controlled by D_Q in the dynamics of the density, and through the coefficients λ_x in the dynamics of the order parameter. $\lambda_C = \frac{f}{\xi}\overline{\lambda}_C$, $\lambda_R = \frac{f}{\xi}\overline{\lambda}_R$, and $\lambda_S = \frac{f}{\xi}(\lambda_2 - \overline{\lambda}_C)$ control the strength of active convection and active torque, and flow-alignment due to active shearing respectively. The term with coefficient $\lambda_E = \frac{f}{\xi}\lambda_1$ also comes from the flow-alignment, and appears as the Laplacian of the nematic order tensor. This term, therefore, acts as a negative Frank elasticity in the dynamics.

Before we proceed with the analysis of our theory, we make the following observations in order to place this model in the context of other the existing literature in this field:

1. The CIDF, introduced by Ramaswamy et. al.[32,33], is the only active contribution to the dynamics which is first order in **Q** and therefore gives a universal description of the behavior of active nematics near the critical density, where **Q** is small. This term gives rise to striking phenomena, such as giant number fluctuations, phase separation, and band formation near the critical density[20,34–45]. In this work we will focus on the dynamics of a system which is well above the critical density and highly ordered, away from this well-studied regime.
2. Existing theories of active nematics that account for the novel defect dynamics seen in these systems consider nematohydrodynamic equations coupled to a Stokes equation for the activity-induced flow (such as[8–14,18]). In the presence of a screening mechanism such as confinement to 2D, the flow field can be eliminated in terms of the active stress yields Eqs. (3–4), but with $D_Q = \lambda_C = \lambda_R$ i.e., a Galilean invariant version of our theory[18,46–48].
3. The approach taken here is one which can be generalized to other active systems. We consider gradient descent on a free energy, in an imposed flow, and allow for broken Galilean invariance. We then replace the general flow with one which depends on the local order parameter, and arises due to the active forces. The same prescription can be applied to polar systems to get the dynamical equations of Toner and Tu[27–29]. The difference being that, in a polar system, the flow from the active forces is $\vec{u}$

$\propto \vec{P}$ where $\vec{P}$ is the polar order parameter. In both cases the gradient descent dynamics are purely smoothing and allow for a homogeneous solution, but the flow which arises due to the motion of those particles, or the forces that they exert, can lead to instabilities in that homogeneous solution, and inhomogeneous dynamical steady states.

Parameters of the Theory

The relaxational contributions to the dynamics of the order parameter arising from a free energy take the form

$$[\partial_t Q_{ij}]_{\mathrm{Eq}} = D_r[\alpha - \beta \mathrm{Tr}\mathbf{Q}^2]Q_{ij} + 2\bar{D}_E \nabla^2 Q_{ij} + \frac{D_\delta}{\rho}\left(2\partial_k(Q_{kl}\partial_l Q_{ij}) - ([\partial_i Q_{kl}]\partial_j Q_{kl})^{\mathscr{T}}\right) + D_\rho(\partial_i\partial_j)^{\mathscr{T}}\rho - K\nabla^4 Q_{ij}$$

where $\alpha = (\rho - 1)$ and $\beta = \frac{1}{\rho^2}(\rho+1)$, D_r is the rotational diffusion constant and D_ρ is a kinetic term also seen in prior works[36,37,41]. There are three elastic terms. $\bar{D}_E$ is the mean elasticity, and it competes with the active term with coefficient λ_E. We will therefore work with an effective mean-elastic relaxation term with coefficient $D_E = \bar{D}_E - \lambda_E$. D_δ is a differential elasticity, measuring the difference between bend and splay energies. Finally, a fourth-order gradient term (with coefficient K) is included to ensure smoothness and numerical stability.

The relevant parameters for the phenomenology discussed are: the active force and torque ($\lambda_{C,R}$) and the effective mean and the differential elastic constants D_E and D_δ. The active shear (with coefficient λ_S) does not affect the linear stability or the phenomenology considered here. In the following, we nondimensionalize our equations by setting our time scale to be the rotational diffusion time, $\frac{1}{D_r}$, and our length-scale to be the diffusion length, $\ell_D \equiv \sqrt{D/D_r}$. In all of the subsequent sections we will work in these dimensionless variables.

Instabilities of the Nematic State

In the homogeneous limit, Eqs. (4) and (3) admit a uni-axial nematic solution with average density $\rho_0 > 1$, and the order parameter $\mathbf{Q} = \rho_0 S_0(\hat{x}\hat{x} - \frac{1}{2}\mathbf{I})$, with degree of ordering $S_0 = \sqrt{\frac{2(\rho_0 - 1)}{\rho_0 + 1}}$. Let us consider spatial fluctuations about this state.

Phase Separation Instability

There is an instability which occurs near the critical density for the onset of ordering, and leads to phase separation. It occurs when fluctuations perpendicular to the director cause an instability in the degree of ordering, which occurs for $D_Q > \sqrt{2(\rho_0^2 - 1)}\left(\frac{\rho_0+1}{\rho_0^2+\rho_0-1}\right)$. This

instability causes phase separation into bands of dense ordered regions coexisting with dilute disordered regions when the material is near the critical density ($\rho_c = 1$). This has been discussed in previous work by us[45] and others[39–41,43,44,49,50]. The nonlinear active terms (λ_C, λ_R and λ_S) do not significantly alter the phenomenology discussed in previous work.

Splay and Bend Instabilities

Let us also consider fluctuations in the direction of order δQ_{xy}. The Fourier transform ($\tilde{X} = \int d\vec{r} e^{i\vec{k}\cdot\vec{r}} X(\vec{r}, t)$) of the linearized equation for this mode can be expressed as

$$\partial_t \delta\tilde{Q}_{xy} = -k^2 \left(2D_E \mp S_0\left(\frac{\lambda_R}{2} - D_\delta\right) + k^2 K\right) \delta\tilde{Q}_{xy}$$

where we consider only pure bend fluctuations which are parallel to the director ($\vec{k} = k\hat{x}$, upper sign) or pure splay fluctuations which are perpendicular ($\vec{k} \cdot \hat{x} = 0$, lower sign). Pure bend and splay decouple fluctuations in the direction of order from those in the degree of order ($\delta\tilde{Q}_{xy}$) and the density ($\delta\tilde{\rho}$) which enables a clear identification of mechanisms at play. This equation reveals two instabilities in the direction of order which come from the activity. Both grow as k^2, and the fourth-order gradient term with coefficient K guarantees that, when there is an instability in this mode, the ordered solution will restabilize at finite wavelength.

The generic instability

This instability occurs when $D_E = \bar{D}_E - \lambda_E < 0$, and it comes from the first order flow-alignment term $\lambda_E = \frac{f}{\xi}\lambda_1$. This instability in the homogeneous nematic occurs for suspensions of extensile rods ($f, \lambda_1 > 0$), which we consider here[¶]. It is a bend (splay) instability when $\lambda_R > 2D_\delta$ ($\lambda_R < 2D_\delta$). The analogous instability has been identified and discussed in detail (in the $D_\delta = 0$ limit) in existing active nematic theories for suspensions[11,13,23,51] and for flows with damping[18].

This instability has also been discussed in the overdamped limit, where it results in a Swift-Hohenberg-type dynamical equation, which can lead to pattern formation, or a turbulent steady-state[19]. The systems with a negative effective elastic constant form steady-state patterns in the modulation of the director for the case of active systems[18,19]. This result is reminiscent of the patterns seen in equilibrium phases of liquid crystals which have a negative elastic constant due to their shape[52–54]. As this instability and its consequences have been the topic of previous theoretical and numerical investigation, we shall forgo further discussion of them here.

Active Torque Instability

Of primary interest here is a bend instability which arises from the active torque. This occurs when a 'bend instability parameter' $\psi = \frac{\lambda_R - 2D_\delta}{D_E \cdot \Lambda(\rho_0)} > 1$ where $\Lambda(\rho_0) = 4\sqrt{\frac{\rho_0 + 1}{2(\rho_0 - 1)}}$ (Fig. 3).

[¶]The generic instability can also occur for contractile discs ($f, \lambda_1 < 0$)

This parameter reflects a competition between the active torque λ_R and the differential elasticity D_δ, which is positive if bend distortions are more energetically expensive than splay. This bend instability is also a mechanism for defect generation and formation of inhomogeneous steady states in this active system. Note that if the nematic was contractile, λ_R is negative and hence there exists a splay instability, which occurs when $\psi < -1$. We have, however, focused on extensile systems for this study of the overdamped dynamics, and left the study of the contractile, overdamped dynamics to future work.

Consequences of the Active Torque

In order to elucidate the consequence of the active torque instability, we numerically explored the dynamics using a semi-implicit finite difference method, with periodic boundary conditions[‖]. Integrating from nematic initial conditions with small amplitude Gaussian noise, two states were found above the threshold for the bend instability ($\psi > 1$). These were (I) an undulating nematic state where the system is strongly ordered but the director undulates along the broken symmetry direction (see Fig. 1, and (II) a turbulent state (see Fig. 3,2) in which charge $\pm\frac{1}{2}$ disclinations continually form and annihilate and the $+\frac{1}{2}$ defects are self-propelled as seen in[4–6,8–10,10–15,51,55].

The structure of the undulating nematic state is reminiscent of twist-bend and splay-bend modulated structures found in equilibrium nematics[52,56,57]. This state present when active convection was large ($\lambda_C > 1.0$) or and it was small ($\lambda_C << 1$) and $D_\delta \leq 0$ (see ESI[†] for details). In other regions of parameter space the system transitioned directly into the defective nematic state.

The above analysis focused on the instabilities of the homogeneous nematic state. Next we consider isotropic initial conditions and vary parameters which control the bend instability (λ_R, D_δ, and ρ_0) and the strength of active convection (λ_C) while keeping the other parameters fixed.

Defect-ordered state

When the strength of active torque is dominant over the strength of active convection ($\lambda_R > \lambda_C$), and $D_\delta > 0$ there is a steady-state with finite defect density *below the bend instability* ($\psi < 1$). This is where the defect-ordered state occurs (see Fig. 4). The properties of this state are as follows: (i) Defects are point-like and the background is a (locally) well-ordered nematic (see Fig. 2). (ii) Defining the orientation of $+\frac{1}{2}$ defects to be opposite the “comet tail” (along the direction of propulsion), we find that these defects exhibit *significant polar ordering*. (iii) The degree of polar ordering decreases as ψ increases. (iv) The high degree of polar ordering corresponds with long splay distortions which are left by $+\frac{1}{2}$ defects as they

[‖]The spatial resolutions (h, units of ℓ_D) used were $0.1 \leq h \leq 0.4$, temporal resolutions were $0.1 \leq \frac{dt}{h^2} \leq 0.4$ diffusion times, and system sizes were between 400 and 1200 ℓ_D

travel (see Fig. 1). Other $+\frac{1}{2}$ defects tend to reorient rather than cross these distortion-trails, leading to long parallel structures which are visible in the states with a large degree of polar ordering.

Turbulent nematic state

The turbulent, defective nematic state occurs above the bend instability when the defect density and vorticity increase sharply (Fig 4). The defects, which were small and circular near $\psi = 1$, become spatially extended and the average degree of ordering decreases. This turbulent nematic state appears distinct from the one arising through the generic bend instability through correlation function $C_\omega(R) = \langle\omega(0)\omega(R)\rangle/\langle\omega^2\rangle$, where $\rho\vec{\omega} = \lambda_R\vec{\nabla} \times (\nabla \cdot \mathbf{Q})$. It scales with the bend instability parameter ψ (see Fig. 5), which is linear in the strength of the active torque λ_R. This differs from what was found in a recent study[13] where vorticity scaled as the strength of the activity to the 1/4th power. Further, if the length scale for defect separation ℓ_d scales with the vorticity $(\ell_d \propto \frac{1}{\psi})$, then the defect density should scale as ψ^2. This is compatible with the trend seen near the critical value of the bend instability parameter, but the range is not large enough for a conclusive comparison.

Summary

We have introduced a universal theory of an overdamped active nematic in which activity enters through self-induced flows. This theory encompasses the physics already identified in previous work and identifies additional phenomena particularly relevant for rigid rod extensile systems. We have identified three nonequilibrium steady states admitted by this theory. The first is a defect-ordered nematic state where polar ordering of +1/2 disclinations emerges from the underlying apolar theory. The theory provides robust predictions about when polar defect ordering will be found. The ordering occurs *below any bend instability*, i.e., $\psi < 1$ and $D_E > 0$ and when $D_\delta > 0$ and $\lambda_R > \lambda_C$. This result implies that an polar ordered fluid phase of defects may not occur in theories which have Galilean invariance ($\lambda_C = \lambda_R$). Other steady states found include an undulating nematic state which is reminiscent of the “walls” of distortion in the order parameter seen before the onset of defective states[11,13], or the distortion of the director which happens during relaxation oscillations[51,58]. Finally we find a turbulent nematic state similar to that which occurs in theories of active nematic suspensions[8–14].

Supplementary Material

Refer to Web version on PubMed Central for supplementary material.

Acknowledgments

We thank Mike Hagan, Zvonimir Dogic, and Stephen DeCamp for sharing information and ideas. EFP and AB acknowledge support from NSF-DMR-1149266, the Brandeis-MRSEC through NSF DMR-0820492 and NSF MRSEC-1206146, NSF PHY11-25915 through KITP, and the HPC cluster at Brandeis for computing time. EFP also acknowledges support through NIH-5T32EB009419 and IGERT DGE-1068620.

References

1. De Gennes, P-G.; Prost, J. The physics of liquid crystals. Vol. 23. Clarendon press Oxford; 1993.
2. Chaikin, PM.; Lubensky, TC. Principles of condensed matter physics. Cambridge Univ Press; 2000.
3. Laverntovich, OD. Soft matter physics: an introduction. Springer; 2003.
4. Sanchez T, Chen DTN, DeCamp SJ, Heymann M, Dogic Z. Nature. 2012; 491:431–434. [PubMed: 23135402]
5. Keber FC, Loiseau E, Sanchez T, DeCamp SJ, Giomi L, Bowick MJ, Marchetti MC, Dogic Z, Bausch AR. Science. 2014; 345:1135–1139. [PubMed: 25190790]
6. DeCamp SJ, Redner GS, Baskaran A, Hagan MF, Dogic Z. Nature Materials. 2015; 14:1110–1115. [PubMed: 26280224]
7. Zhou S, Sokolov A, Lavrentovich OD, Aranson IS. Proc. Nat. Acad. Sci. U.S.A. 2014; 111:1265–1270.
8. Giomi L, Bowick MJ, Ma X, Marchetti MC. Phys. Rev. Lett. 2013; 110:228101. [PubMed: 23767749]
9. Thampi SP, Golestanian R, Yeomans JM. Phys. Rev. Lett. 2013; 111:118101. [PubMed: 24074119]
10. Blow ML, Thampi SP, Yeomans JM. Phys. Rev. Lett. 2014; 113:248303. [PubMed: 25541809]
11. Giomi L, Bowick MJ, Mishra P, Sknepnek R, Marchetti MC. Phil. Trans. R. Soc. A. 2014; 372:20130365. [PubMed: 25332389]
12. Thampi SP, Golestanian R, Yeomans JM. Phys. Rev. E. 2014; 90:062307.
13. Thampi SP, Golestanian R, Yeomans JM. Phil. Trans. R. Soc. A. 2014; 372:20130366. [PubMed: 25332382]
14. Thampi SP, Golestanian R, Yeomans JM. Europhys. Lett. 2014; 105:18001.
15. Shi, X-q; Ma, Y-q. Nat. Commun. 2013; 4:3013. [PubMed: 24346733]
16. Saintillan D, Shelley MJ. Phys. Rev. Lett. 2007; 99:058102. [PubMed: 17930796]
17. Saintillan D, Shelley MJ. Phys. Rev. Lett. 2008; 100:178103. [PubMed: 18518342]
18. Doostmohammadi A, Adamer MF, Thampi SP, Yeomans JM. Nat. Commun. 2016; 7:10557. [PubMed: 26837846]
19. Oza AU, Dunkel J. eprint arXiv:1507.01055. 2015
20. Narayan V, Ramaswamy S, Menon N. Science. 2007; 317:105–108. [PubMed: 17615353]
21. Kemkemer R, Kling D, Kaufmann D, Gruler H. Eur. Phys. J. E. 2000; 1:215–225.
22. Duclos G, Garcia S, Yevick HG, Silberzan P. Soft Matter. 2014; 10:2346–2353. [PubMed: 24623001]
23. Ramaswamy S, Rao M. New J. Phys. 2007; 9:423.
24. Lavrentovich, O.; Kleman, M. Chirality in Liquid Crystals. Springer; 2001. p. 115-158.
25. Renn SR, Lubensky TC. Phys. Rev. A. 1988; 38:2132.
26. Beris, AN.; Edwards, BJ. Thermodynamics of flowing systems: with internal microstructure. Oxford University Press; 1994.
27. Toner J, Tu Y. Phys. Rev. Lett. 1995; 75:4326–4329. [PubMed: 10059876]
28. Toner J, Tu Y. Phys. Rev. E. 1998; 58:4828–4858.
29. Toner J, Tu Y, Ramaswamy S. Annals of Physics. 2005; 318:170–244.
30. Farrell FDC, Marchetti M, Marenduzzo D, Tailleur J. Phys. Rev. Lett. 2012; 108:248101. [PubMed: 23004336]
31. Gopinath A, Hagan MF, Marchetti MC, Baskaran A. Physical Review E. 2012; 85:061903.
32. Simha R, Ramaswamy S. Physica A. 2002; 306:262–269.
33. Ramaswamy S, Simha RA, Toner J. Europhys. Lett. 2003; 62:196–202.
34. Mishra S, Ramaswamy S. Physical Review Letters. 2006; 97:090602. [PubMed: 17026350]
35. Chaté H, Ginelli F, Montagne R. Phys. Rev. Lett. 2006; 96:180602. [PubMed: 16712353]
36. Baskaran A, Marchetti MC. Phys. Rev. E. 2008; 77:011920.
37. Baskaran A, Marchetti M. Phys. Rev. Lett. 2008; 101:268101. [PubMed: 19113789]

38. Mishra S, Aditi Simha R, Ramaswamy S. J Stat. Mech. Theory Exp. 2010; 2010:P02003.
39. Peruani F, Ginelli F, Bär M, Chaté H. J. Phys. Conf. Ser. 2011; 297:012014.
40. Peshkov A, Ngo S, Bertin E, Chaté H, Ginelli F. Phys. Rev. Lett. 2012; 109:098101. [PubMed: 23002888]
41. Peshkov A, Aranson IS, Bertin E, Chaté H, Ginelli F. Phys. Rev. Lett. 2012; 109:268701. [PubMed: 23368625]
42. Baskaran A, Marchetti MC. Eur. Phys. J. E. 2012; 35:95. [PubMed: 23053844]
43. Bertin E, Chaté H, Ginelli F, Mishra S, Peshkov A, Ramaswamy S. New J. Phys. 2013; 15:085032.
44. Ngo S, Peshkov A, Aranson IS, Bertin E, Ginelli F, Chaté H. Phys. Rev. Lett. 2013; 113:038302.
45. Putzig E, Baskaran A. Phys. Rev. E. 2014; 90:042304.
46. Pismen LM. Phys. Rev. E. 2013; 88:050502.
47. Srivastava P, Marchetti MC. Private Commnication. 2015
48. Srivastava, P.; Marchetti, MC. Instabilities and patterns in an active nematic film. APS March Meeting; 2015.
49. Ginelli F, Peruani F, Bär M, Chaté H. Phys. Rev. Lett. 2010; 104:184502. [PubMed: 20482178]
50. Ngo S, Ginelli F, Chaté H. Phys. Rev. E. 2012; 86:4–8.
51. Giomi L, Mahadevan L, Chakraborty B, Hagan MF. Nonlinearity. 2012; 25:2245.
52. Dozov I. Europhys. Lett. 2007; 56:247–253.
53. Panov VP, Nagaraj M, Vij JK, Panarin YP, Kohlmeier A, Tamba MG, Lewis RA, Mehl GH. Phys. Rev. Lett. 2010; 105:15–18.
54. Ponti S, Freire FCM, Dias JC, Evangelista LR. Phys. Lett. A. 2008; 372:6521–6526.
55. Gao T, Blackwell R, Glaser MA, Betterton M, Shelley MJ. Phys. Rev. Lett. 2015; 114:048101. [PubMed: 25679909]
56. Meyer R. Les Houches summer school in theoretical physics. 1973:273–373.
57. Shamid SM, Dhakal S, Selinger JV. Phys. Rev. E. 2013; 87:1–11.
58. Giomi L, Mahadevan L, Chakraborty B, Hagan MF. Phys. Rev. Lett. 2011; 106:218101. [PubMed: 21699344]

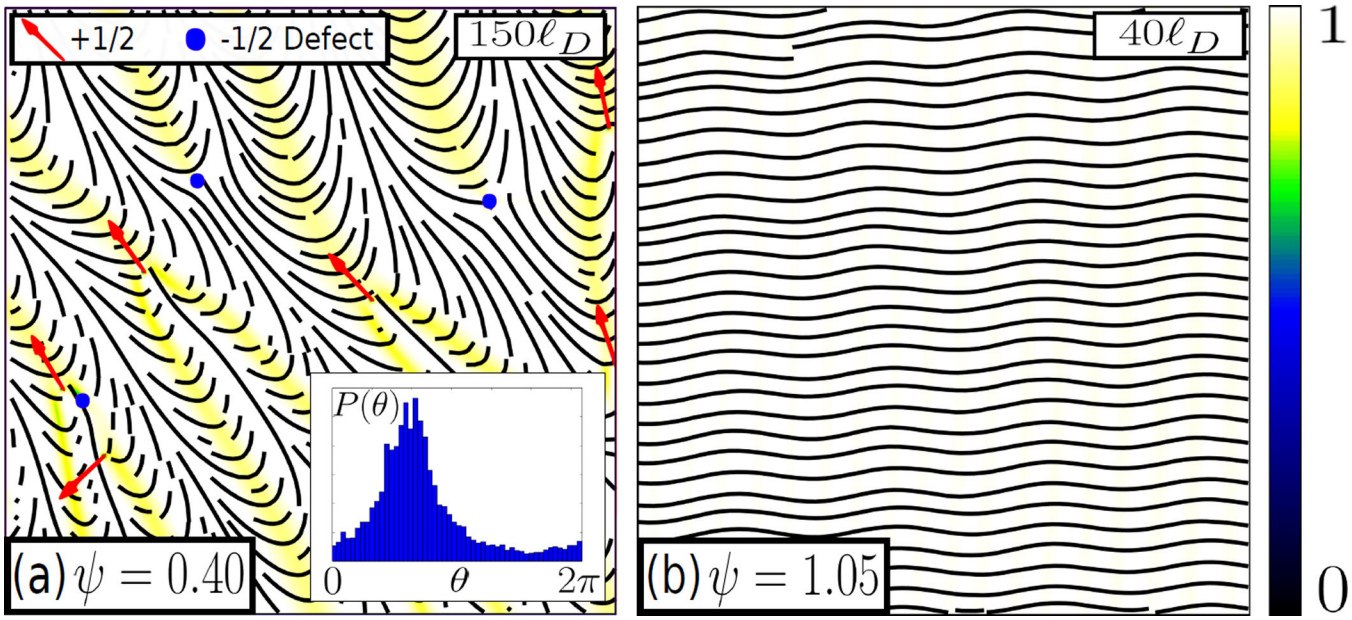

Fig. 1.

Heatmaps of the degree of order (S/S_0, colorbar on the right) showing the nonequilibrium steady-states. (a) The defect-ordered state, with a histogram inset showing the sharp polar ordering in the orientation of $+\frac{1}{2}$ defects. The lines, showing the direction of order, highlight the extended trails left by the motion of these defects. (b) The undulating nematic state is highly ordered ($S \simeq S_0$) but the direction of order undulates. Scale bars are in the top right corners.

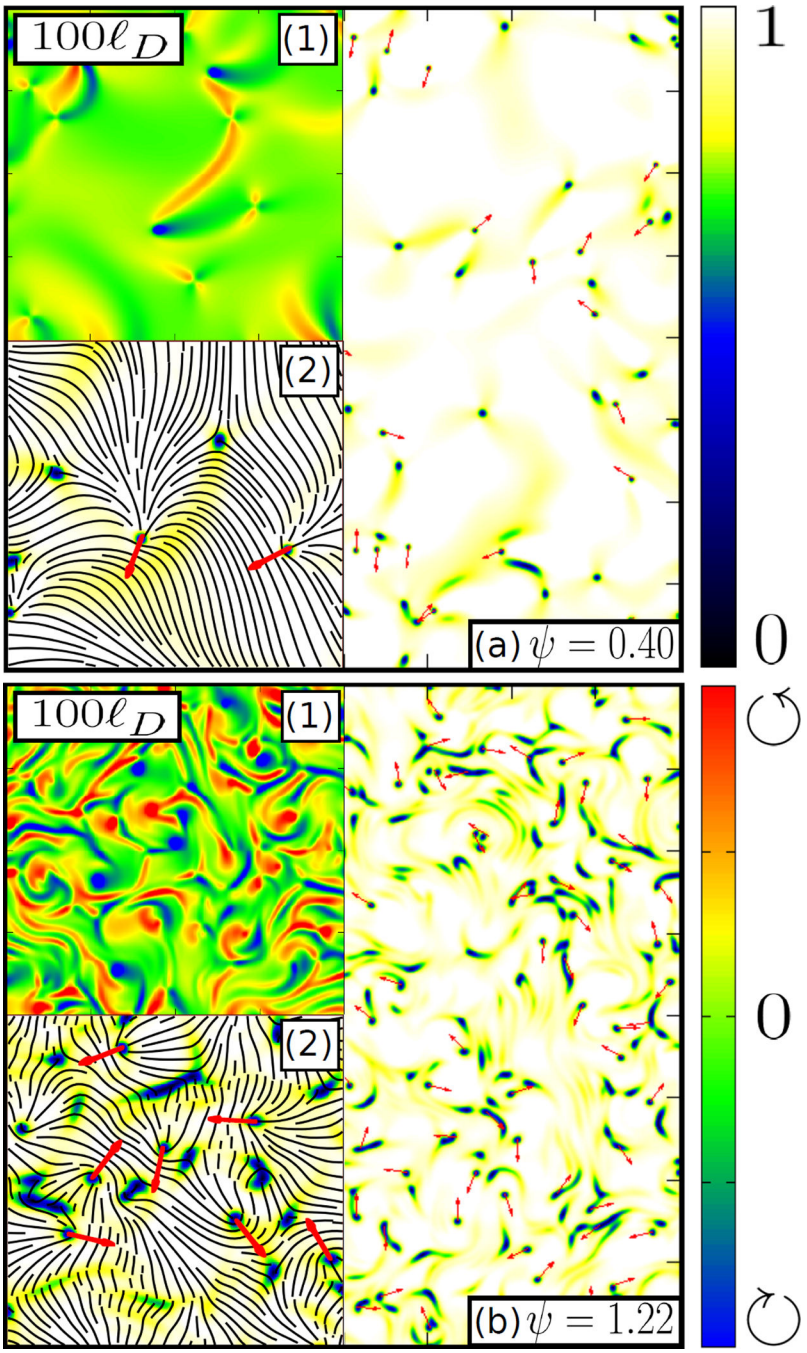

Fig. 2.

Heatmaps of the degree of order (S/S_0, colorbar on the upper-right) showing the defective states (a) at low activity ($\psi < 1$) and (b) at high activity ($\psi > 1$). Insets on each heatmap include (1) a heatmap of the vorticity (colorbar on the lower-right), and (2) 2×-magnified region with lines showing the direction of order. Scale bars are in the top left corners.

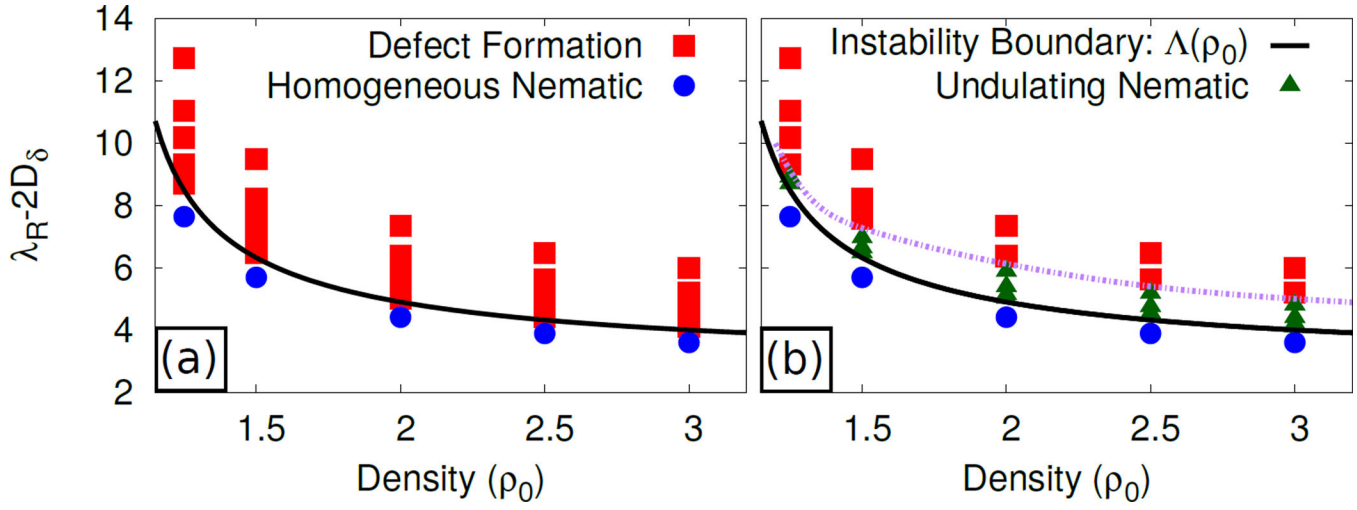

Fig. 3.

Plots showing the end state which forms from nematic initial conditions. (a) At $D_\delta = 1.0$, the homogeneous nematic state transitions into a defective nematic above the instability boundary. (b) At $D_\delta = -0.50$ we find an undulating state at intermediate activities.

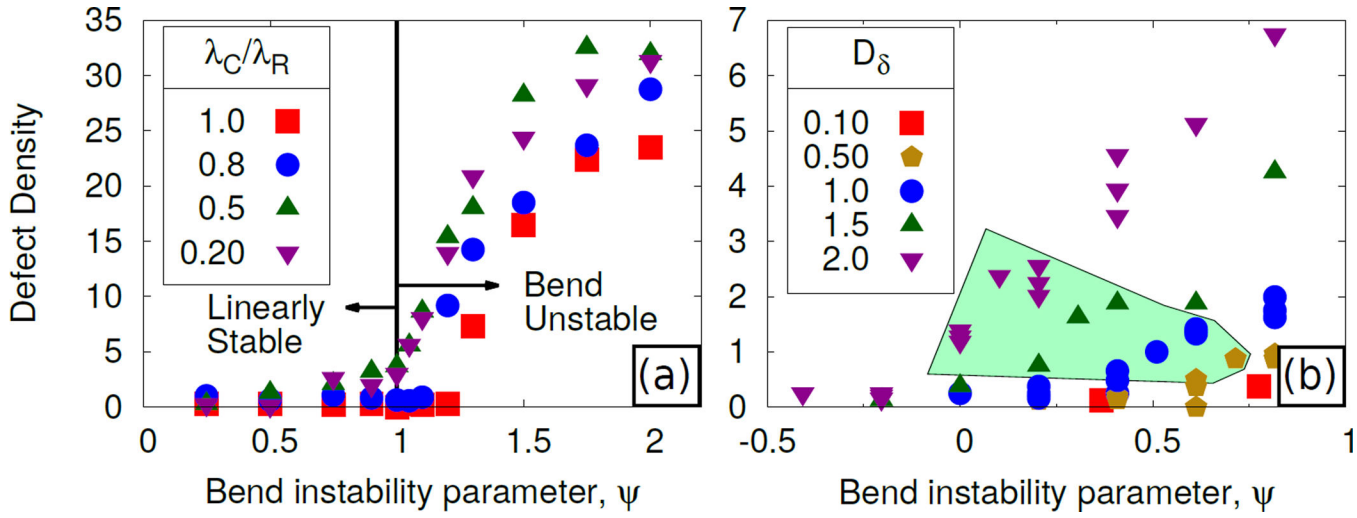

Fig. 4.

Plots of the defect density (defects per $(100\ell_D)^2$) as a function of ψ, for $\rho_0 = 2.0$. (a) Curves with fixed $D_\delta = 1.0$, for a range of λ_C/λ_R, show that when the strength of active convection is comparable to active torque, defects vanish near the bend instability. When $\lambda_C < \lambda_R$ the defect density can be nonzero for $\psi < 1$, in which case it increases sharply when ψ crosses 1, and then saturates. (b) Fixed $\lambda_C = 1.0$ (less than λ_R), and a range of D_δ, for $\psi < 1$. Defect density is greater for larger D_δ, and it vanishes as D_δ goes to 0. The shaded region indicates where there was statistically significant polar ordering of $+\frac{1}{2}$ defects.

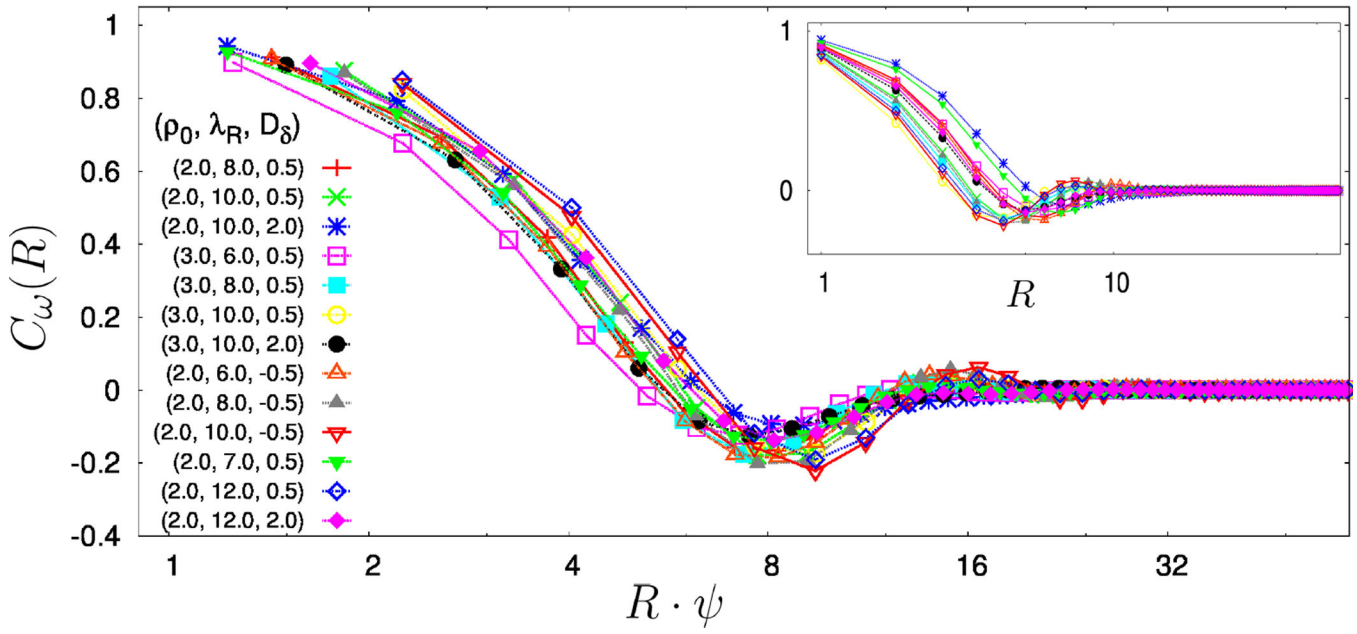

Fig. 5.

Log-linear plot of vorticity correlation functions, $C_\omega(R)$ for fixed parameters (λ_R, D_δ and ρ_0) above the bend instability ($\psi > 1.10$). The length is scaled by ψ, which gives a data collapse for a large range of parameters.